1. Introduction

Carbon nanostructures with pore size down to nanometer scales are of great importance. They can be either in form of crystalline carbon nanoparticles (CNPs) or, e.g., highly porous nanostructured carbon xero- or aerogels. The most important representatives of CNPs are fullerenes, carbon nanotubes (CNTs), graphenes and their derivatives. These materials have high mechanical strength, chemical stability and most of them are considered non-toxic, even biocompatible. The key question of both of their applications in a biological context or their behaviour in natural environment (i.e., in water) is their hydrophobic-hydrophilic property. The interaction of carbon materials with water is a double-sided phenomenon. Hydrophilicity is disadvantageous when water competes with the adsorptive that is to be removed, but it is desirable in several situations, e.g., in electrochemical, biological or environmental applications.

The projects involved three groups: The plasma chemistry group from HAS RCNS (Hungarian Academy of Sciences, Research Centre of Natural Sciences), the surface chemistry group from BME (Budapest University of Technology and Economics) and the environmental colloid group from University of Debrecen.

2. Plasma assisted incorporation of nitrogen functionalities into carbon nanoparticles

Our goal was the preparation and modification of carbon nanoparticles, both their morphology and surface chemistry mostly by plasma technology. Characterization and description of the obtained carbon materials were performed by classical sorption and scattering techniques using the most advanced evaluation methods.

Commercial and lab made samples were used in these experiments. The improved Hummers' synthesis of graphene oxide (GO) from graphite was used to prepare GO for this project. It was investigated to monitor how the functional groups form during the synthesis steps. To achieve these, samples were taken after every preparation step and analysed with TG-DTA/MS, FTIR, XRD and SEM-EDX techniques. It was found that the main characteristic mass loss step of GO was around 200 °C, where at first the carboxyl and lactone groups were released. The evolution of sulfonyl groups followed them right away in a partially overlapping step. It became clear that in the as-prepared acidic GO sample the presence of H_2SO_4 originating from the reaction solution was still dominant. The functional groups were formed only after washing the as-prepared GO with HCl. The reduction of the GO structure back to reduced GO resulted in the loss of the functional groups, and a graphitic material was obtained back [N. Justh, B. Berke, K. László, I. M. Szilágyi: *Journal of Thermal Analysis and Calorimetry*, (131) 2267–2272, **2017**].

Graphene-type nanoparticles were successfully doped with nitrogen by using nitrogen plasma treatment (**Figure 1**). Surface chemical alterations were followed by X-ray photoelectron spectroscopy (XPS). The applied treatments resulted in a significant build-up of nitrogen in the surface of these nano-carbon materials. The amount of nitrogen varied between 4 and 10 atomic %, depending on type of carbon and on biasing conditions. Peak component at 398.3 eV is assigned to C=N-C type, at 399.7 eV to sp(2) N in melamine-type ring structure and at 400.9 eV to N substituting carbon in a graphite-like environment. [Bertóti, M. Mohai, Cs. Balázsi, K. László, J. Szépvölgyi: *Open Chem*. (13) 451-456, **2015**]. Also multilayer graphene (MLGR), its bulk analog and highly oriented pyrolytic graphite (HOPG) were treated by radio frequency activated low pressure N_2 gas plasma (at negative bias 0-200 V, for 5-20 min). Surface composition and chemical-state alterations were delineated by X-ray photoelectron spectroscopy (XPS) as well. Covalently bonded nitrogen of 5-15 at% incorporated into the surface. The higher N concentration in MLGR below 100 V is attributed to the larger number of defects. In-depth distribution of N restricted to 2-4 monolayers. Model calculation resulted in 23 at% N (at 100 V) in the top graphene layers of HOPG. [I. Bertóti, M. Mohai, K. László: *Carbon*, (84) 185-196 **2015**].

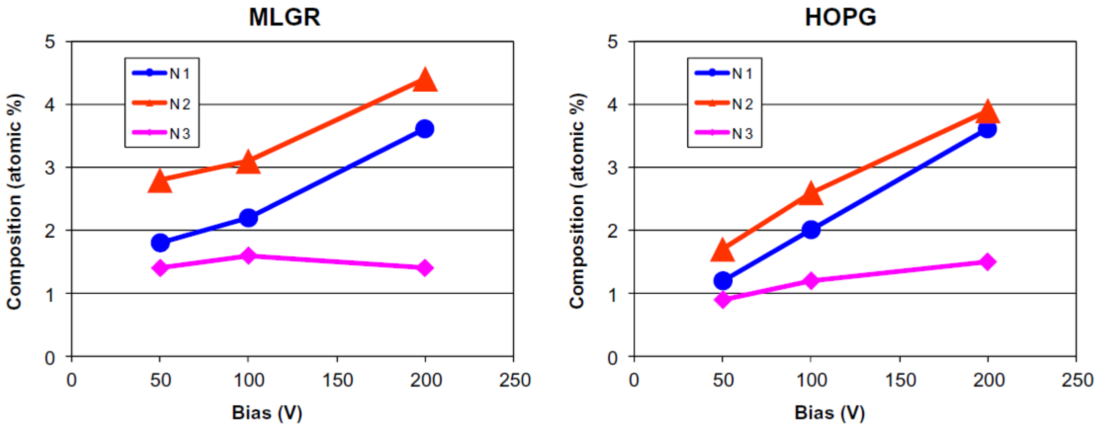

Figure 1. Development of nitrogen functionalities is influenced by the accelerating voltage in the plasma reactor. N1: sp^2 N in pyridine type ring, N2: sp^2 N in pyrrole, diazine or triazine type ring structure, N3: N substituting C in graphite plane

In international collaboration, by a new active screen plasma treatment we could reduce graphene oxide. A transparent graphene oxide layer on a non-conductive poly(ethylene terephthalate) film was treated at temperatures ranging from 100°C to 200°C in pure hydrogen and in a gas mixture of hydrogen and nitrogen. UV-visible absorption spectra, X-ray diffraction, Raman spectra, X-ray photoelectron spectra (XPS) and electrical properties confirmed that the graphene oxide could be effectively reduced by the active screen plasma treatments. Detailed XPS quantitative analyses have revealed that the carboxylic groups are not stable, and their amount can be decreased effectively by the active screen plasma treatments. Only about one third of the carbonyl type C=O can be reduced at the same time. In addition to the reduction, non-intentional simultaneous multi-element doping of GO with nitrogen from the gas supply and with Fe, Cr and

Mo from the stainless steel active screen was also detected by XPS [J. Chen, X. Shi, S. Qi, M. Mohai, I. Bertóti, Y. Gao, H. Dong: *Carbon* (95) 338-346, **2015**].

We performed glow discharge N_2 or Ar plasma treatments of thin layers of graphene oxide (GO) deposited from slurry in alcohol onto stainless steel substrates as well. The treatment was performed in the preparation chamber of the x-ray photoelectron spectrometer, allowing reliable in situ characterization of the treated surface by quantitative x-ray photoelectron spectroscopy. Approximately 10 atomic % nitrogen was incorporated into the graphene oxide surface. Further increase of N-content resulted in decrease of the O content from the starting value of 29 to similar to 15 atomic %. The high resolution C1s, O1s, and N1s spectra show several different chemical states. It was established that the carboxyl-type and the carbonyl-type C-O clusters were more affected by both plasma treatments as their amount was selectively eliminated. [M. Mohai and I. Bertóti: *Surf. Interface Anal*. (48), 461–464, **2016**]**.** An interesting applications of the plasma reactor was to prepare gold nanoparticles from crystalline gold salt. Beyond the value of this result we are proud of working with the late professor Mihály T. Beck in this project. [M.T. Beck, I. Bertóti, M. Mohai, P. Németh, E. Jakab, L. Szabó, J. Szépvölgyi: *Journal of Solid State Chemistry* (246) 65–74, **2017**]

3. The role of carbon surface chemistry in various applications

3.1. Confinement or surface chemistry?

We characterised the *hydrogen diffusion* in a resorcinol-formaldehyde based carbon aerogel. Neutron and X-ray scattering analyses revealed no long range graphitic ordering in the material, but a hierarchical structure above the nanometre length scale. We observed a highly accelerated ortho-para conversion of the spin isomer states of the hydrogen molecule, which can be explained by the large number of available electron donors at the carbon aerogel surface. We also observed a partial hindrance of the conversion that we linked to hindered rotations due to the narrow confinement in ultramicropores with a pore diameter of less than 7 Å. The percentage of non-converted hydrogen agrees well with the relative available surface area in these ultramicropores [E. Bahn, O. Czakkel, B. Nagy, K. László, S. Villar-Rodil, J.M.D. Tascón, F. Demmel, M.T.F. Telling, P: *Carbon* (98), 572-581, **2016**].

In applications involving organic vapor, the performance of high surface area carbons is often challenged by water vapor in the atmosphere. The high surface area carbon in which the pore sizes are of the order of a few nanometers was exposed to an atmosphere containing simultaneously a model aromatic molecule, toluene, and water vapor. Small angle neutron scattering (SANS) combined with contrast variation was found to be a powerful means of investigating the behavior of otherwise immiscible toluene−water mixtures in confined conditions. Unlike what happens with pure toluene vapor, and in spite of its high surface oxygen content, when the carbon is exposed to pure water vapor, surface wetting by the adsorbate is incomplete. The existence of water-free surfaces even at relative humidity (RH) 100% provides direct evidence that the film of adsorbed water is discontinuous and that, by corollary, the water molecules form clusters on the carbon surface and the density of the adsorbed water is lower than that in the bulk liquid. When toluene is also present, all the available carbon surface is wetted. Toluene and water adsorb as a single phase already at relative humidity (RH) 11.5%, and the concentration of water present in the adsorbed phase is as high as 2.9 wt %, far above its solubility in bulk toluene (0.033 wt % at 25 °C) Figure 2).

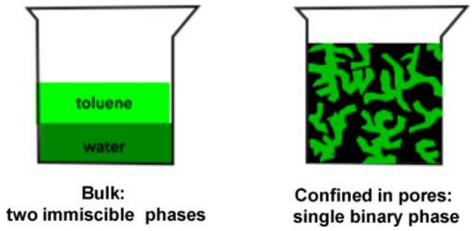

Figure 2. The effect of pore confinement on the miscibility of toluene – water mixtures

At RH 87% the concentration of water in the adsorbed phase is four times higher, approximately 12 wt %. The recently proposed mechanism of anchoring of the water by the aromatic molecules may provide an explanation for this phenomenon [K. László, B. Demé, O. Czakkel, E. Geissler: *J. Phys. Chem. C* 118 (41), 23723–23727 **2014.**]

3.2. Role of surface chemistry, implications for relevant applications

3.2.1. Interaction with proteins

Using small angle neutron and X-ray scattering (SANS and SAXS) adsorption of proteins (bovine serum albumin (67 kDa), and bovine pancreatic trypsin inhibitor (BPTI)(6.5 kDa)) on two carbon substrates were studied. One of them was an open structured carbon aerogel C1 (derived from a resorcinol-formaldehyde polymer aerogel by us) and a commercial nanoporous carbon C2 (Figure 3).

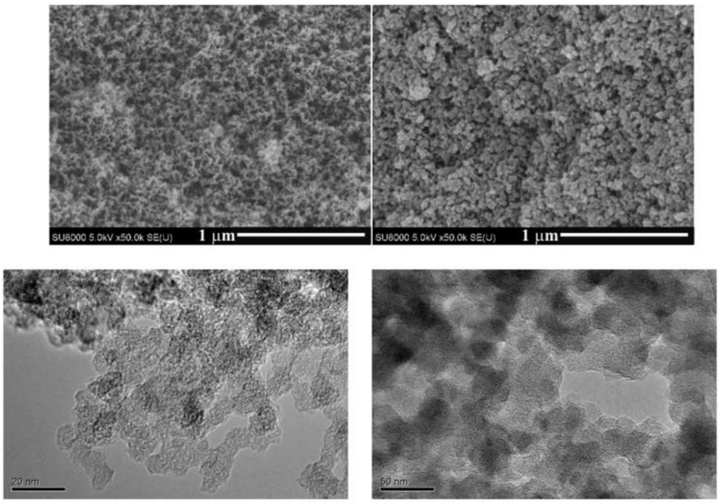

a b

Figure 3. SEM and HRTEM images of the C1 (a) and C2 (b) carbon samples. Scale bars in the HRTEM images are 20 nm and 50 nm for C1 and C2, respectively.

In C1, which is hydrophobic, the BSA molecules migrate individually into pores that are compatible with their size, whereas BPTI forms clusters having the same size as BSA. With C2, the hydrophilic internal surface limits the adsorption efficiency (**Figure 4**). The strong adhesion of proteins to hydrophilic surfaces prevents diffusion of either molecule into the micro-and nanopores. These observations have relevance to biomedical applications, such as haemoperfusion or as a medium for protein storage. [B. Nagy, A. Tóth, I. Savina, S. Mikhalovsky, L. Mikhalovska, I. Grillo, E. Geissler, K. Laszló: *Carbon* (106), 142-151 **2016**].

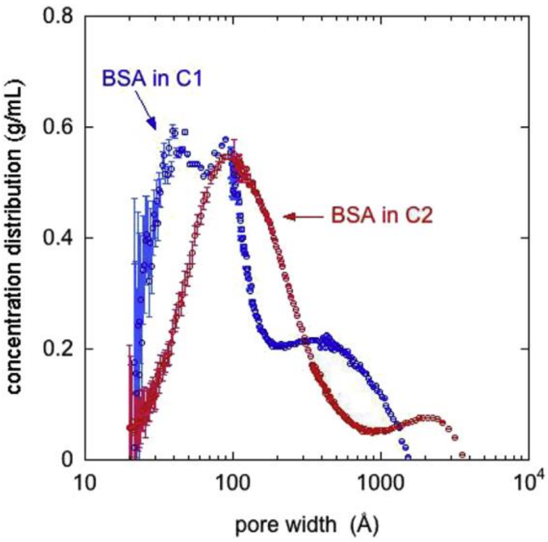

Figure 4. Concentration distribution BSA in the C1 and C2 carbon particles plotted as a function of pore width. The cut-off at high q occurs in both samples at q ≈ 0.31 $Å^{-1}$. (The trend c(q)→0 at q < 0.01 $Å^{-1}$ in C1 is an artefact from the excess surface scattering of C1 in pure D_2O.)

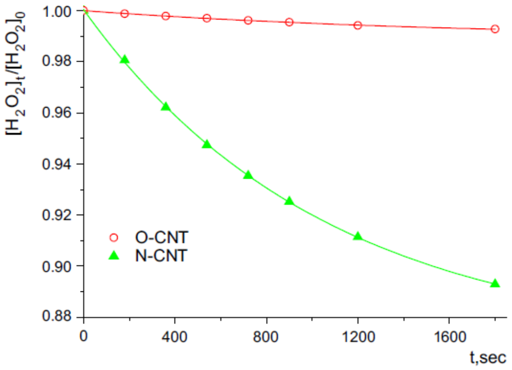

Figure 5. Kinetic curves comparing the H_2O_2 decomposition activity of O and N doped CNTs at 293 K, pH ≈ 8.0.

3.2.2. Enzyme mimetic catalysis

The carbon nanotubes (CNTs) are effective catalysts of decomposition of hydrogen-peroxide. We have shown, by means of experimental and quantumchemical tools, that both the lowest calculated activation energy (similar to 18.9 kJ/mol) and the highest rate constant correspond to the N-containing CNTs (**Figure 5**). The calculated chemisorption energy values correlate with the operation stability of multi-wall (MW) CNTs. Based on the proposed quantum chemical model it was found that the catalytic activity of carbon materials in electron transfer reactions is controlled by their electron donor capability. [K. Voitko, A. Tóth, E. Demianenko, G. Dobos, B. Berke, O. Bakalinska, A. Grebenyuk, E. Tombácz, V. Kuts, Y. Tarasenko, M. Kartel, K. László: *Journal of Colloid and Interface Science* (437) 283–290, **2015**].

3.2.3. Enhanced electrocatalytic activity

Building sulphur heteroatoms into carbon aerogel a metal free oxidation-reduction catalyst could be prepared. Resorcinol-formaldehyde base carbon aerogels treated at high temperature resulted in a catalyst with electron transfer number close to 4e$^-$ and the onset potential for the oxygen reduction reaction was shifted to a more positive value. [M. Seredych, K. László, J. T. Bandosz: *ChemCatChem 7* (18) 2924-2931 **2015**]. Composites of carbon aerogel and graphite oxide (GO) were also synthesized using a self-assembly method based on dispersive forces. Their surface was modified by treatment in hydrogen sulfide at 650 and 800 °C. The synergistic effect of the composite (electrical conductivity, porosity and surface chemistry) leads to a good oxygen reduction reaction catalytic activity. The onset potential for the composite of carbon aerogel heated at 800 °C is shifted to a more positive value and the number of electron transfer was 2e(-) at the potential 0.68 V versus RHE and it increased to 4e(-) with an increase in the negative values of the potential. An excellent tolerance to methanol crossover was also recorded. [M. Seredych, K. László, E. Rodriguez-Castellon, T.J. Bandosz: *Journal of Energy Chemistry* (25), 236-245 **2016)**

Using melamine as nitrogen source resorcinol (R)-melamine (M)-formaldehyde (RMF) polymer gels were also prepared. The M/R molar ratio varied in the range 0-1. Thus, the nitrogen content was tuned in the 0-4 % region. The deduced pore volume decreases with increasing N content. At the highest M concentration a different microscopic structure than the usual set of 3D beads developed **(Figure 6**).

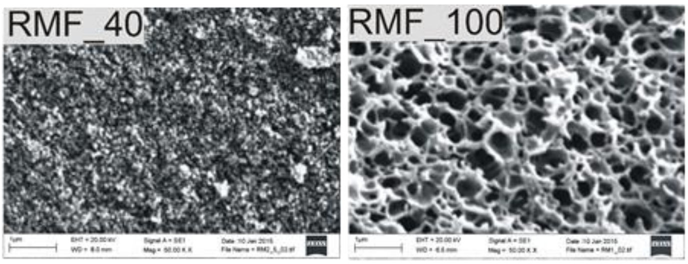

Figure 6. SEM images of carbon aerogels. The usual 3D bead structure (see Figure 3a) was found in the M/R< 0.4, while a much opener structure formed in M/R =1 conditions

The carbon matrices obtained possess not only complex porosity but a heterogeneous distribution of the functional groups: both O and N heteroatoms are less abundant on the surface than in the bulk. The M/R ratio increases not only the N but also the O content of RMF based carbon samples. Both N1s and O1s XPS spectra could be deconvoluted into bands from three species. N is found at the surface predominantly in the form of pyridine like structures and as condensed polyaromatic systems where N substitutes C, while O is in single and double bonds with carbon atoms. Although the carbon surface became less hydrophobic as the concentration of the heteroatoms increased, the accessibility of the pores becomes limited, due probably to blocking by the large amounts of N and O. Cyclic voltammetry (CV) gave reasonable test results. The monotonically increasing onset potential of oxygen reduction reaction approaches that of a ply-acryl-nitrile derived carbon in our sample with 4% N content. The good correlation found between the cathode current densities relative to the BET surface area reveals that the accessibility of the N species is an important factor in the electrocatalytic process (**Figure 7**) [B. Nagy, S. Villar-Rodil, J.M.D. Tascon, I. Bakos, K. László: *Microporous and Mesoporous Materials* (230), 135-144, **2016**].

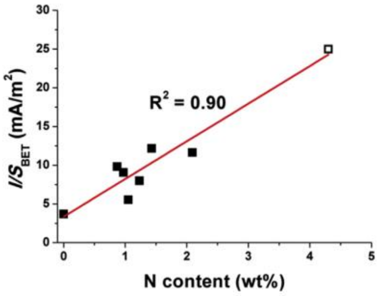

Figure 7. Influence of bulk nitrogen content on cathodic current densities at 0.05 V (vs RHE) normalized to the BET surface area of carbon

Catalytic efficiency of this nitrogen-doped, mesoporous carbon aerogel cathode catalyst was also investigated in a two-chambered microbial fuel cell (MFC) applying graphite felt as base material for cathode and anode, utilizing peptone as carbon source. This mesoporous carbon aerogel containing catalyst layer on the cathode increased the maximum power density normalized to the anode volume to 2.7 times higher compared to the maximum power density obtained applying graphite felt cathode without the catalyst layer. Besides the increase of the power and the rate of biodegradation, the investigated catalyst decreased the internal resistance. Although Pt/C catalyst proved to be more efficient, a considerable decrease in the material costs might be achieved by substituting it with nitrogen-doped carbon aerogel in MFCs. Such cathode still displays enhanced catalytic effect [G. M. Tardy, B. Lóránt, M. Lóka, B. Nagy, K. László: *Biotechnology Letters*, 39 (7):993-999 **2017]**.

4. Potential of NMR in studying nanostructured materials and their surface interactions

In this part of the project we encountered a second but insolvable difficulty. The set up the solid state NMR could not be installed at University of Debrecen. The two main reasons were the technical error in the newly set up NMR consol and the economical restriction which first locked then distracted our saved sources for this purpose. Finally decided to concentrate on the development of non-standard liquid state NMR method and on the low-resolution NMR relaxometry.

The implementation of the NMR cryoporometry for soft materials had to be solved. We tested our NMR cryoporometry protocol on silica aerogels with known pore size distributions from nitrogen adsorption. The NMR cryoporometry brought pore size distribution in the mesoporous range and was superior to nitrogen sorption when the silica aerogel was doped organic gelatine. The cryoporometry results served a good starting point the new type description of adsorption-desorption kinetics of a model drug on this aerogel. [P. Veres, M. Kéri, I. Bányai, I. Lázár, I. Fábián, C. Domingo, J. Kalmár: *Colloids and Surfaces B* (152) 229-237, **2017**].

In studying carbon compounds after promising start with cryoporometry we met some difficulties. First we found that our cryoporometry method is not enough sensitive to the surface modified carbons. As we wrote above, that the heteroatoms modified only a very thin layer of the surface, no effect could be detected by NMR. Therefore we turned to the parallel characterization of the morphology of different porous carbons aerogels prepared by the Surface Chemistry (BME) group. As a good start resorcinol-formaldehyde (RF) aerogels (**Figure 3a**) we could get good agreement with the nitrogen adsorption experiments. However, after carbonization the two methods sharply deviated. The nitrogen adsorption unequivocally showed micropores with decrease size compared to the starting RF aerogel. While it was hidden for the NMR cryoporometry, only slit like mesopores were detected. A tentative explanation is that the micro-pores are so hydrophobic that the water could not get into that under the circumstances of cryoporometric experiment. Later these results appeared again therefore we accepted that the *sorption experiments are strong for micropores while the NMR cryoporometry for the the* *mesopores*. The alteration of the cryoporometric solvents to less hydrophilic ones can partially extend the method to reach smaller pores in case of hydrophobic substrates. For the prepared RF carbon aerogels we implemented the "cryoporometric titration" method, we studied the melting/freezing curves by adding water step by step. In **Figure 8** the results of these titrations are shown.

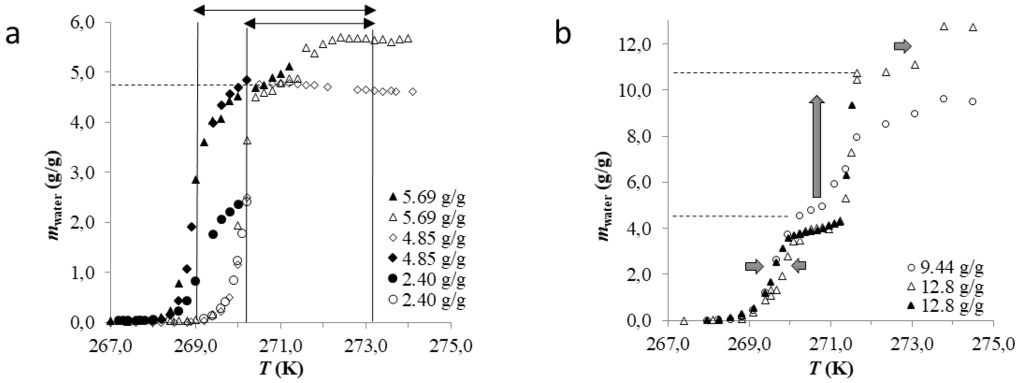

Figure 8. Melting and freezing curves of RF carbon aerogel: a) 2.4-5.69 g/g filling level, where lines and with double arrows show the melting and freezing point depressions, b) 9.44-12.8 g/g filling level, where dashed lines show the saturation levels of different pore types, while arrows denote the observed shifts. Empty symbols stand for the melting, while filled for the freezing processes.

From **Figure 8** we can see two characteristic temperatures of phase transitions and in picture (a) with a melting/freezing hysteresis. From these results the meso pore-distribution could be drawn as it is in **Figure 9**.

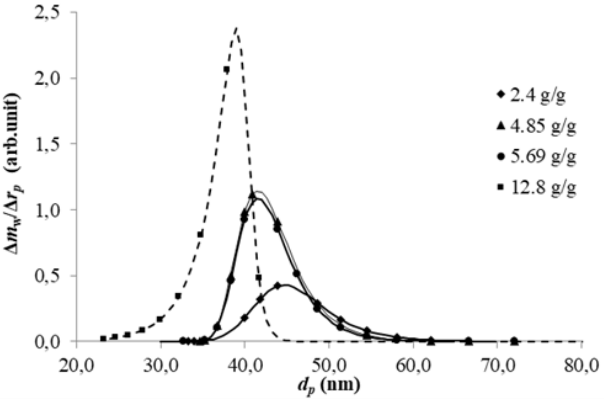

Figure 9. Pore size distributions in RF carbon aerogel at different filling states. Solid lines stand for the spherical pores, while dashed line for the cylindrical ones.

From the hysteresis we stated that there are spherical and cylindrical pores of 40 nm and 38 nm respectively. Nitrogen adsorption experiments showed high micro-porosity (the sorption curve started at 200 cm^3/g at the lowest pressure), and prose size distribution about 2-3 nm. Indications of presence of mesopores are also shown in N_2-sorption curves but with no characteristic distribution curves. It is important to note that the cryoporometric titration impresses that the filling of the pores happens in the way that first the spherical pores load water then the channels, which interconnect them. [M. Kéri, I. Bányai, D. Nyul, B. Nagy, K. László: *Parallel NMR cryoporometry, relaxometry and diffusiometry studies of porous carbon aerogels,* Book of Abstracts, Interpore2018 New Orleans]

The mechanism of wetting was further confirmed by low-field NMR relaxometric titration experiments. The change the transverse relaxation time as a function of the water content is shown in **Figure 8**.

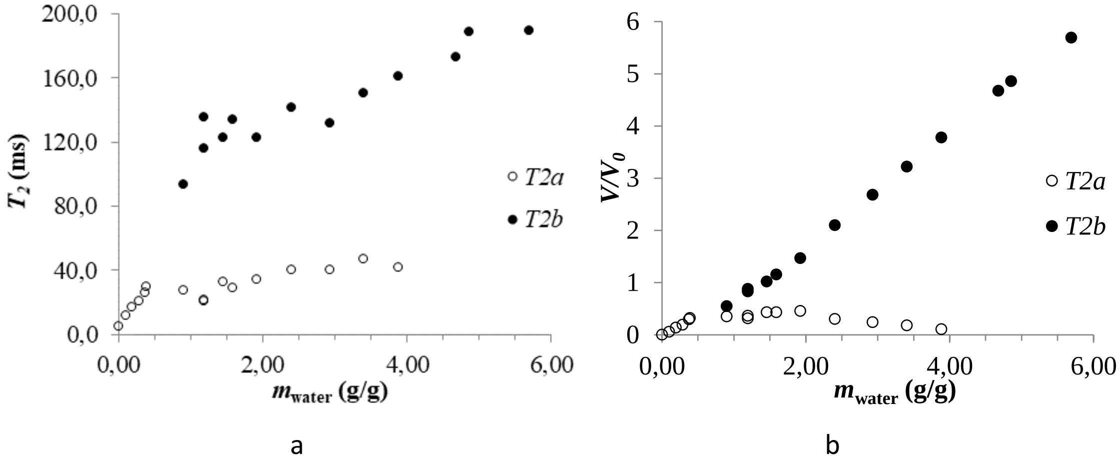

Figure 9 Transverse (*T_2*) relaxation times (a) and the volume of water at each compartment compared to the given whole volume (b) as a function of the water content in 1g of carbon aerogel

With the complex interpretation of these results we can obtain information about the wetting mechanism of the aerogel. Below about 0.5 g/g water content only one relaxation process can be observed **(Figure 9a**), T_{2a} with empty symbols), with increasing transverse relaxation time and amplitude. The lack of a constant, low T_2 value means that no continuously increasing hydration layer forms on the surface, thus this relaxation process can be attributed to the increasing number of water molecules adsorbed on the hydrophilic groups of the carbon backbone. Above filling of ca. 1 g/g all these function groups are hydrated completely, showing T_2 between 25 – 45 ms and constant volume (**Figure 9a**, empty symbols). At 0.9 g/g filling state a longer T_2 component (**Figure 9a** T_{2b}) appears, indicating water molecules which are less affected by the restricted motion near the surface or the interactions with the solid material. In our explanation water gradually fills out the pores of the structure after each other, resulting in slightly increasing T_{2b} (from about 120 to 160 ms) and linearly increasing V/V_0 (**Figure 9b**). At the point $m_{water} \approx 2$ g/g the amount of water related to the short T_2 component gets decreasing, as a part of the hydrated groups is incorporated into the pore-water. Above 4 g/g filling state most of the molecules bound to the surface groups get exchanged covered with the bulk-like molecules in the pores, which accounts for the disappearance of the short T_2 component. From both experiment we could determine the porosity for 40 nm spherical mesopores as about 5g water/1 g carbon aerogel and NMR is in accordance with the sorption experiments.

NMR diffusiometry is a unique tool for study of solution structure and dynamics. The reason is that no chemical potential gradient is needed to observe the diffusion, the experiments can be made in a very simple way. This simplicity drives users to collect data under not well controlled circumstances and to draw false conclusions. Our goal was to use this method in proper way to study interactions between small molecules (usual content of our solution phase experiments: water, phosphate buffer, organic solvents) and big molecules or surfaces of porous materials. Starting with model systems we could determine the hydrated structure micellar systems by measuring the diffusion of water molecules hindered by the micelles. The constructed model described well the earlier made small angle neutron scattering experiments [I. Bányai, I. Lakatos, G. Meier, Z. Nagy, Sz. Vass: *Bull. Chem. Soc. Jpn*. (90) 854-862, **2017**].

In real solid/liquid systems the constant pH is very important. To achieve it the most often applied buffer is the phosphate and it considered as an innocent anion. Its specific interaction with the target molecules or surfaces is rarely considered. Using a very symmetric and regularly branching macromolecule, fifth generation polyamido-amine-dendrimer (G5_PAMAM.NH_2) we tested two important features of the planned NMR methods. With ^{31}P-NMR diffusiometry (and 2D multinuclear methods) we proved the residence of phosphate ions in the macromolecular phase, identified the bonding sites within the macromolecule. This macromolecule in solid from can adsorb water. Using this fact, by means ^{1}H-cryoporometry we determined the size of the cavities in this soft “porous” macromolecules. [M. Kéri, Z. Nagy, L. Novák, E. Szarvas, L. P. Balogh P, I, Bányai: Phys. Chem. Chem. Phys (19) 11540-11548, **2017**]. These studies based on that unique feature of NMR that the relaxation times (transversal and longitudinal) are in the same order of magnitude to the molecular motions and the time scale of equilibrium chemical reactions. We published two papers about this statement. One is a perspective [I. Bányai: *New Journal of Chemistry* (42) pp. 7569-7581 **2018**] in which we summarized the correct experimental and evaluation methods for application of dynamic NMR. The other was an application of NMR diffusiometry and solid state NMR (performed at Pannon University, Veszprém) in order to prove the change of size and geometry of poly-tungstate cluster from solid state to solution. The contribution of our project is in the Acknowledgment of this paper. [W. W. Ayass, T. Fodor, E. Farkas, Z. Lin, H. M. Qasim, S. Bhattacharya, A. S. Mougharbel, K. Abdallah, M. S. Ullrich, S. Zaib, J. Iqbal, S. Harangi, G. Szalontai, I. Bányai, L. Zékány, I. Tóth, U. Kortz: *Inorganic Chemistry* (57) *pp.* 7168-7179 **2018]**.

Armed with the knowledge of the interpretation of NMR diffusiometry the motion of the water in carbon aerogels were investigated using with titration method. The results became surprising.

We had two NMR peaks but the smaller one was omitted in the cryoporometry experiments because it did not freeze.

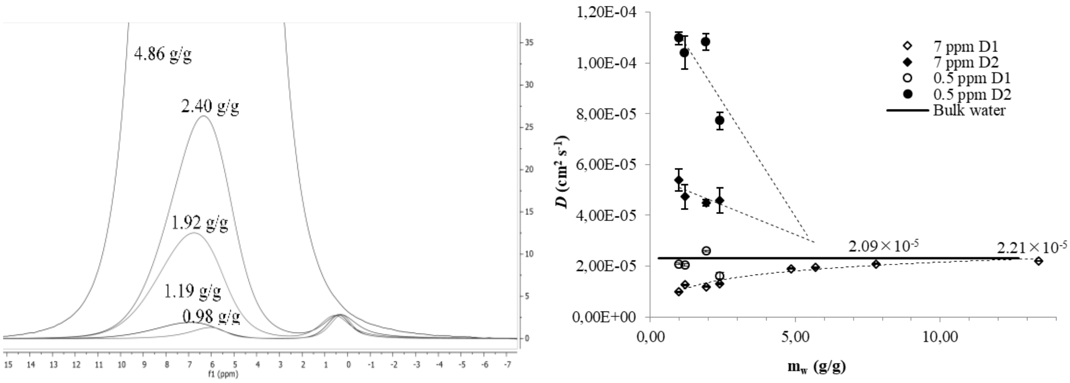

a b

Figure 10. NMR spectra of water in RF carbon aerogel (left) and the diffusion coefficients of water in RF carbon aerogel as a function of the water content at 298 K (right). The solid line shows the theoretical value of bulk water ($2.3 \cdot 10^{-5}$ cm^2s^{-1}), while dashed lines are only for guiding the eyes

Diffusion measurements could have been performed for *both* peaks (at lower water contents) and found bi-exponential decay (a slow and a fast diffusion) of the stimulated echo intensity as a function of the square of amplitude of gradient pulse. For the dominant peak of pore-filling water (~7 ppm) the slow diffusion has *D* value of ca. 1 10^{-9} m^2s^{-1} compared to *D* of free water (2.3 10^{-9} m^2s^{-1}). With increasing the water content this apparent diffusion coefficient increases and at higher water content it reaches the bulk value. The fast component is about 5.4 10^{-9} m^2 s^{-1} and decreases with the increasing water content and becomes not observable from about 5 g/g concentration. Considering the studies literature we attributed the presence of “fast” components to the vapor phase diffusion of water which can exist exclusively in the partially filled samples. When we reach the complete filling of mesopores it disappears. As **Figure 10b** shows the saturation value is about 5g water/g aerogel as we found with cryoporometry and relaxometry. The same behavior is observed for the smaller peak (**Figure 10**) but the “slow” component has larger diffusion coefficient as D =2 10^{-9} m^2 s^{-1}, while the diffusion coefficient of “fast” component” is extremely large, $D \approx 1$ 10-8 m^2 s^{-1} and decreases steeply with the water content. A manuscript reporting these results is under preparation [M. Kéri, I. Bányai, D. Nyul, B. Nagy, K. László: Parallel NMR cryoporometry, relaxometry and diffusiometry studies of porous carbon aerogels*,* for *Carbon,* in manuscript form, 2018].

Using room temperature ionic liquids (RTILs) as a novel solvent could also enhance the tuneability of these porous structures of carbon aerogels (CAs). RTILs added at low concentration (< 3 m/m % in the initial water based solution) have been used as a template to tune RF based CAs

[Yang, H. et al. (2012). *J. Mater. Chem*. 22, 21852-56.]. Ionic liquids, however, were expected also to act as catalyst and/or reactant.

The following alkyl-substituted imidazolium based RTILs mixed with various amounts of water were used in the reactions: 1 ethyl-3-methylimidazolium acetate ([emim][ac]), 1-butyl-3-methylimidazolium acetate ([bmim][ac]), 1-ethyl-3-methylimidazolium ethyl sulfate ([emim][EtSO4]) and 1-ethyl-3-methylimidazolium methyl sulfate ([emim][MeSO4]). As the polymerization also took place in the absence of any added acidic or basic catalyst, results showed that [emim][EtSO4] indeed acted as catalyst, on the contrary, N and S content – if any – of the samples were below the detection limit of the XPS method. The advantage however of using RTILs as solvent is, that both the type of the RTIL and the water content of the RTIL/water mixture strongly influence the morphology and the pore structure of the CAs (**Figure 11**). Two manuscripts reporting our results on polymers and carbon aerogels of ionic liquid tuned porosity are under preparation [Balázs Nagy, Krisztina László: Room temperature ionic liquid porogens to tailor resorcinol-formaldehyde polymer aerogels; László et al: Ionic liquid tuned mesoporous carbon aerogels].

.

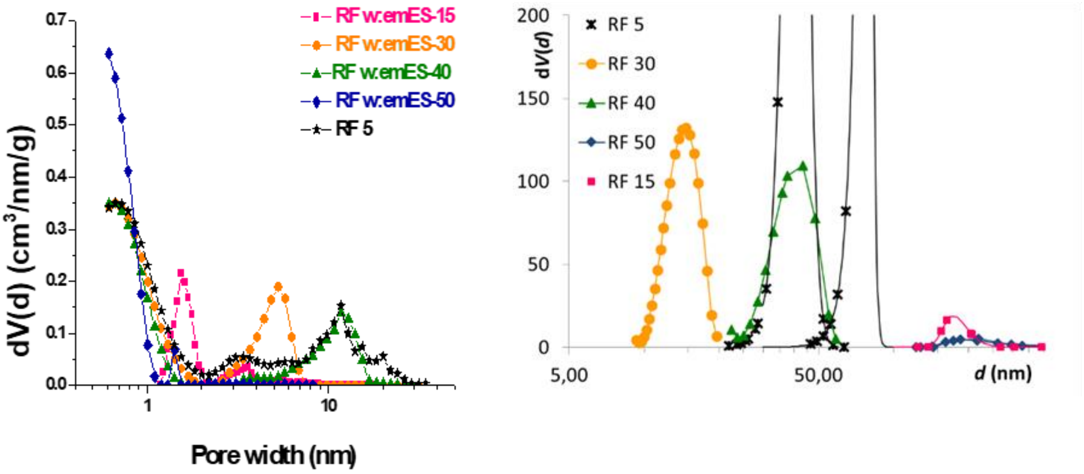

Figure 11. Pore size distributions from N$_2$-adsorption (left) and NMR cryoporometry (right). The evaluation for sorption experiments were QSDFT with slit geometry, while for NMR spherical and cylindrical geometry. CAs prepared a) in different RTILs. Black: [emim][MeSO4], red: [emim][EtSO4], blue: [emim][ac], green: [bmim][ac], magenta: only water; and b) in [emim][EtSO4]/water medium. Red: 9% water, olive: 15 % water, green: 20 % water, brown: 25 % water, black: 31 % water, purple: 37 % water, blue: 43 % water, yellow: 49 % water, magenta: 55 % water (unpublished results)

Figure 11 reveals that the N$_2$-sorption and NMR show the same tendency. The scales are dramatically different. We are making now a great effort to synchronize the results. At the present state of speculation is that for the blue and red cryoporometry and N$_2$-sorption see different range of pores. For the rest the same argument could be use but we try to suggest at least one alternative explanation before publication.

5. Conclusions

Within this project completely succeeded the following goals.

- Succesful preparation of more than one dozen heterogenized (N, O, ans S atoms) carbon nanosystems: graphenes, graphene-oxides, carbon aerogels.
- By means of plasma technology the large surface modification was achieved. Using mainly X-ray photoelectron spectroscopy and self-developed evaluation methods detailed characterization of the modified carbons was succeeded.
- The surface modified carbon nanosystems found applicable for reduction-oxidation catalysts.
- N-doped carbon aerogels were also prepared in chemical route and tested as electrode materials. We studied the sorption properties and the diffusion of small molecules in it by neutron scattering and NMR techniques.
- Dynamic NMR methods were implemented for structure analysis of systems containing nanoparticles in liquid and solid phase.
- RF-carbon aerogels were synthetized wit tunable pore size. The morphology was determined in dry state by N_2-adsoprtion methods in wet state (in action) by means of NMR cryoporometry, relaxometry and diffusiometry.
- The synchronization of gas/vapor adsorption and NMR methods is very important result of the project although it has not been achieved completely. It attracts an industrial interest beyond the novelty in basic research.

The research groups from three important research centres cooperated according to expectations. Especially the synergy between the HAS-RCNS Plasma Chemistry and the BME Surface Chemistry groups furthermore between the latter and UD Environmental Colloid groups worked out very fruitfully.